Applied Catalysis B: Environmental 163 (2015) 547–553

Contents lists available at ScienceDirect

Applied Catalysis B: Environmental

journal homepage: www.elsevier.com/locate/apcatb

Enhancement of visible light mineralization ability and photocatalytic activity of $BiPO_4$/BiOI

Yanfang Liu[a], Wenqing Yao[a], Di Liu[a], Ruilong Zong[a], Mo Zhang[a], Xinguo Ma[b], Yongfa Zhu[a,*]

[a] Department of Chemistry, Beijing Key Laboratory for Analytical Methods and Instrumentation, Tsinghua University, Beijing 100084, China
[b] School of Science, Hubei University of Technology, Hubei 430068, China

ARTICLE INFO

Article history:
Received 12 June 2014
Received in revised form 8 August 2014
Accepted 22 August 2014
Available online 30 August 2014

Keywords:
$BiPO_4$/BiOI
Photocatalysis
Mineralization ability
Charge transfer

ABSTRACT

Visible light mineralization ability is of great importance for the practical use of a photocatalyst. As a promising visible light photocatalyst, BiOI has relatively weak mineralization ability and is not efficient enough for the removal of some organic pollutants. In this work, the visible light mineralization ability of BiOI was improved via charge transfer between $BiPO_4$ donor and BiOI acceptor. This charge transfer in $BiPO_4$/BiOI composite photocatalyst produced more oxidative holes than that produced by pure BiOI, thus significantly improved its mineralization ability. Under visible light ($\lambda > 420$ nm) irradiation, the most effective $BiPO_4$/BiOI could degrade phenol to small molecular organic acids more rapidly than BiOI and its removal efficiency for phenol and TOC were about 2 and 4 times as high as that of pure BiOI, respectively. The enhancement of photocatalytic performance is attributed to the enhanced oxidation ability of the hole and the increased separation and migration efficiency of photogenerated electrons and holes, which is resulted from the relatively large dipole moment of $BiPO_4$.

1. Introduction

The application of photocatalysis in environmental remediation has drawn increasing interest owing to its environmentally friendly merit [1–3]. It can been used in various aspects, such as self-sterilizing, self-cleaning, water purification, air purification, anti-fogging, heat transfer and heat dissipation and so on [4]. Traditional photocatalyst-TiO_2 has many merits, including its low cost, high efficiency and excellent stability. However, it cannot absorb visible light and suffers from fast recombination rate of the photogenerated charge carriers. In order to overcome these drawbacks, much attention has been given to new types of photocatalysts. Of special interest is the visible light active Bi-based photocatalysts [5–8]. Recently, He et al. [9] have made a thorough review on the Bi-based photocatalysts. It covers their type, preparation method, morphology control, composite construction and their properties. Among the Bi based photocatalysts, Bi oxyhalides have anisotropic layered structures with $[Bi_2O_2]^{2+}$ layers intercalated by X^- ions (X = F, Cl, Br, I). The internal electric field that forms between the $[Bi_2O_2]^{2+}$ and X^- layers can promote the separation of photoinduced electrons and holes and thus enhances their photocatalytic activity. Among the Bi oxyhalides, BiOI has the smallest band gap and has been proved to be an efficient visible light photocatalyst for the degradation of RhB [10] and Methyl Orange (MO) [11]. So it is a very promising photocatalyst. However, BiOI exhibited the lowest visible light activity toward the oxidation of NO, indicating the poor oxidation ability of its photogenerated holes [12]. The oxidation ability is one of the most crucial factors that determine whether a photocatalyst can be applied in practical application, especially in water purification, since the formation of certain intermediates in the degradation process of some pollutants will induce higher toxicity than the original pollutant. A case in point is hydroquinone, which is one of the degradation intermediates of phenol and has much higher toxicity than the latter [13]. Furthermore, compared with many UV light photocatalysts, the photocatalytic activity and the mineralization efficiency of BiOI toward organic pollutants are much lower. Therefore, the photocatalytic activity and the mineralization efficiency of BiOI must be improved for its application in industry.

The coupling of a broad band gap semiconductor with a narrow one is a good method to take advantage of both the two semiconductors. If the two semiconductors possess matched energy level, synergistic effect may be achieved. High utilization efficiency of solar energy can be harvested by the narrow band gap

* Corresponding author. Tel.: +86 10 6278 7601; fax: +86 10 6278 7601.
E-mail address: zhuyf@mail.tsinghua.edu.cn (Y. Zhu).

http://dx.doi.org/10.1016/j.apcatb.2014.08.039
0926-3373/

semiconductor; at the same time, low recombination rate of electrons and holes can be realized by the interaction of the two semiconductors. Therefore, it is an efficient method to improve the photocatalytic activity of BiOI [14–22]. $BiPO_4$ is an excellent UV light photocatalyst with strong mineralization ability toward phenol [23–25]. In the past few decades, several narrow band gap semiconductors such as C_3N_4 [26,27], CdS [28], Ag_3PO_4 [29] and $BiVO_4$ [30] were coupled with $BiPO_4$, and it was found that the photocatalytic activities of the composites were significantly improved under visible light. Chen et al. [31] prepared BiOI/$BiPO_4$ hetero-junction by deposition–precipitation method and it was found that BiOI/$BiPO_4$ photocatalyst displayed much higher photocatalytic performance for the degradation of MO than pure $BiPO_4$ and BiOI under visible light. However, it is not easy to obtain a uniform composite by deposition–precipitation method and it will hinder the junction to exert its effectiveness if too much BiOI covers $BiPO_4$. Besides, the improvement of the mineralization ability of BiOI still remains a problem.

This work intends to take advantage of the high efficiency and strong mineralization ability of $BiPO_4$ and the dramatic visible light absorption ability of BiOI, thus obtain a highly efficient visible light photocatalyst with strong mineralization ability. $BiPO_4$/BiOI composite photocatalyst was synthesized via an anion exchange method, and the effect of $BiPO_4$ on the photocatalytic performance of $BiPO_4$/BiOI composite photocatalyst was systematically investigated.

2. Experimental

2.1. Synthesis of the photocatalysts

BiOI was synthesized through a hydrothermal process. All chemicals used were analytic grade reagents. 1.94 g $Bi(NO_3)_3{\cdot}5H_2O$ and 0.830 g KI were dissolved in 80 mL ethylene glycol, respectively. Then KI solution was added into $Bi(NO_3)_3$ solution and the mixture was stirred for 10 min and then transferred into a 200 mL Teflon-lined stainless steel autoclave and maintained at 160 °C for 6 h. The products were washed for one time with ethanol and three times with distilled water and dried at 120 °C for 8 h. $BiPO_4$/BiOI was synthesized via an anion exchange method. 0.176 g BiOI was dispersed in 30 mL distilled water. Then the beaker was placed in an ultrasonic bath for 10 min and was magnetically stirred for 5 min to form a homogeneous suspension at room temperature. Subsequently, certain amount of NaH_2PO_4 (0.1 M) solution was added into the solution. The mixture was stirred for 10 min and then transferred into a 45 mL Teflon-lined stainless steel autoclave and maintained at 180 °C for 24 h. The products were washed three times with distilled water and dried at 120 °C for 8 h.

2.2. Characterization of the photocatalysts

Morphologies of the prepared samples were examined with transmission electron microscopy (TEM) by a Hitachi HT 7700 electron microscope operated at an accelerating voltage of 100 kV. High resolution transmission electron microscopy (HRTEM) images were obtained by a JEOL JEM-2011F field emission transmission electron microscope with an accelerating voltage of 200 kV. The X-ray diffraction (XRD) was performed on a Bruker D8-advance X-ray diffractometer at 40 kV and 20 mA for monochromatized Cu Kα ($\lambda = 1.5418$ Å) radiation. UV–vis diffuse reflectance spectra (DRS) of the samples were measured by using Hitachi U-3010 UV-vis spectrophotometer.

2.3. Photocatalytic reactivity test

The photocatalytic activities were evaluated by the decomposition of phenol under visible light ($\lambda > 420$ nm). Visible light irradiation was obtained from a 500 W Xe lamp (Institute for Electric Light Sources, Beijing) with a 420 nm cut off filter. 25 mg of photocatalyst was dispersed in an aqueous solution of phenol (50 mL, 25 ppm). Before irradiation, the suspensions were first ultrasonicated for 10 min and then stirred for 1 h to ensure adsorption-desorption equilibrium between the catalysts and phenol. At certain time intervals, 3 mL aliquots were sampled and centrifuged to remove the particles. The concentration of phenol was analyzed by recording the absorbance at the characteristic band of 270 nm using a Hitachi U-3010 UV-vis spectrophotometer. To investigate the active species generated in the photocatalytic degradation process, trapping experiments of free radicals (hydroxyl radical and hole) by tert-butyl alcohol (t-BuOH) and ethylenediamine tetraacetic acid disodium salt (EDTA-2Na) were carried out, respectively. N_2 was purged to confirm whether superoxide radical is the main active species. Since the trapping agent (EDTA-2Na) could interfere the UV spectrum of phenol, the concentration of phenol was detected by HPLC instead. The detection condition was as follows: Venusil XBP-C18 (250 mm × 4.6 mm i.d., 5 μm) reversed phase column was used. The mobile phase was a mixture of methanol and water (60:40, v/v) with a flow rate of 1.0 mL min^{-1}. The UV detector was operated at 270 nm. Total organic carbon (TOC) analyzer (Multi N/C 2100, Jena) was employed for mineralization degree analysis of phenol solution. The photocurrents and electrochemical impedance spectra (EIS) were measured on an electrochemical system (CHI-660D, China). A standard three-electrode cell with a working electrode (as-prepared photocatalyst), a platinum wire as counter electrode, and a standard calomel electrode (SCE) as reference electrode were used in the photoelectric studies. 0.1 M Na_2SO_4 was used as the electrolyte solution. The visible light irradiation was obtained from a 500 W Xe lamp with a 420 nm cut off filter.

3. Results and discussion

3.1. Characterization of $BiPO_4$/BiOI composite photocatalyst

$BiPO_4$/BiOI composite photocatalyst was obtained through an anion exchange method. With a much smaller K_{sp}, $BiPO_4$ is more stable than BiOI. Therefore, it is possible for $BiPO_4$ to swap out BiOI, and form on the BiOI sample. As shown in the TEM images, the pure BiOI was nano-sheet (Fig. 1a). When PO_4^{3-} was used to exchange the anion of BiOI, nanorods emerged on BiOI nano-sheet. Besides, as the addition of PO_4^{3-} increased, the amount of nanorods formed on BiOI increased. It can be seen from the HRTEM images (Fig. S1a), the lattice fringes of $BiPO_4$ and BiOI coexisted in $BiPO_4$/BiOI composite. The measured interplanar spacings of 0.1997 nm and 0.3066 nm corresponded to the (200) plane of BiOI and the (120) plane of $BiPO_4$. This revealed that the nanorods formed on BiOI were $BiPO_4$. When the mole content of $BiPO_4$ took up 10% of $BiPO_4$/BiOI composite, the characteristic peak of phosphorous can be obviously observed in EDS (Fig. S1b). This further proved the formation of $BiPO_4$ on BiOI. As the amount of nanorods formed on BiOI increased, the contact area of $BiPO_4$ and BiOI in the composite photocatalyst would increase. However, when the mole content of $BiPO_4$ took up more than 7% of $BiPO_4$/BiOI composite, the size (mainly the diameter) of $BiPO_4$ nanorod would increase with further increasing the additive amount of PO_4^{3-}. This led to the increase of whole volume as well as the remaining volume of $BiPO_4$ that had no contact with BiOI, whereas the contact area of $BiPO_4$ nanorods with BiOI would not increase that much. Therefore, for a certain amount of $BiPO_4$ nanorods, the ratio of their contact area with BiOI to their whole volume (or mass) will decrease as they become larger (wider in diameter). In addition, as shown in TEM images (Fig. 1e), larger $BiPO_4$ nanorod was inclined to grow out of the BiOI nanosheet, making the contact area of $BiPO_4$ and BiOI decrease further.

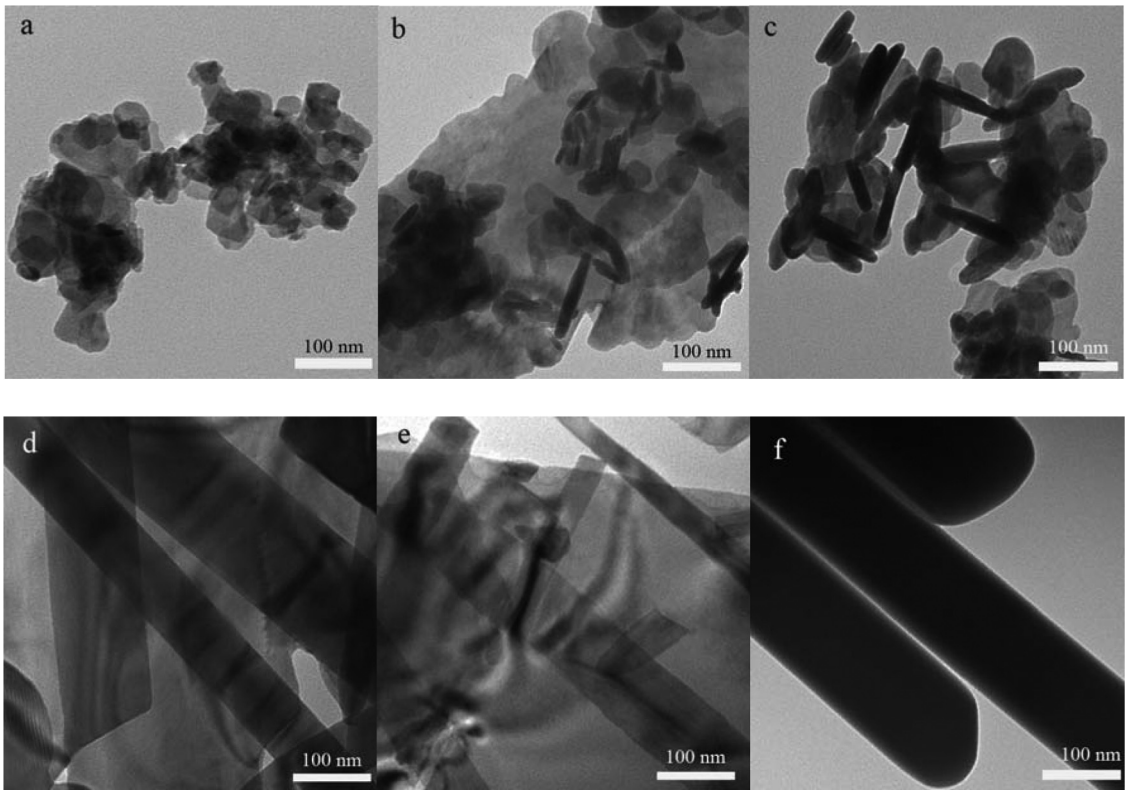

Fig. 1. TEM of $BiPO_4$/BiOI with different content of $BiPO_4$: (a) 0%, (b) 3%, (c) 7%, (d) 10%, (e) 15%, and (f) 100%.

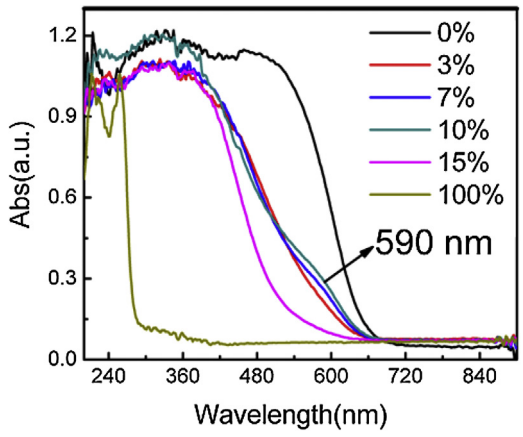

Fig. 2. UV–vis DRS of $BiPO_4$/BiOI with different content of $BiPO_4$.

As shown in the XRD patterns of pure BiOI and $BiPO_4$/BiOI (Fig. S2), apart from the characteristic peaks of tetragonal phase BiOI (JCPDS No. 73-2062), two new peaks corresponding to the monoclinic phase $BiPO_4$ (JCPDS No. 15-0767) emerged in $BiPO_4$/BiOI samples. Besides, as the addition of PO_4^{3-} increased, the (120) peak of $BiPO_4$ became sharper and intenser, which further proved that the amount of $BiPO_4$ formed on BiOI increased and its crystallization was improved.

Fig. 2 showed the effect of $BiPO_4$ on the absorption spectrum of $BiPO_4$/BiOI composites. It can be seen that the existence of $BiPO_4$ decreased the absorption intensity of the composite and led to a blue shift of the absorption edge. Moreover, as the content of $BiPO_4$ increased, the amplitude of blue shift increased. Besides, there was an obvious broad additional absorption peak in the range of 520–620 nm (the peak was at about 590 nm) in $BiPO_4$/BiOI composites (7% and 10%). This absorption peak might result from the charge transfer between $BiPO_4$ and BiOI. Charge transfer absorption is a common phenomenon between electron acceptor and electron donor. It is most commonly seen in complexes consisting of transition metal ions and ligands [32,33]. UV–vis DRS can be used to observe the formation of charge transfer in complexes [34–36]. This can also be applied in the charge transfer between two compounds. In such cases, the electron acceptor can be an organic compound or a halogen compound; and the electron donor can be an inorganic or organic compound [37–40]. In a charge transfer process, one electron transfers from the HOMO (Highest Occupied Molecular Orbital) of the electron donor to the LUMO (Lowest Unoccupied Molecular Orbital) of the closely connected electron acceptor, resulting in the charge transfer absorption. As in metal complexes, the energy for charge transfer transition in composite photocatalysts will be small if the electron acceptor possesses stronger ability to accept electrons or the electron donor possesses stronger ability to give electrons. This might be the case for $BiPO_4$/BiOI composite. In this composite photocatalyst, the electron donor is $BiPO_4$, whose valence band consists of Bi 6s and O 2p. As is reported [41], the coupling between Bi 6s and O 2p produces anti-bonding Bi 6s states toward the top of the valence band and this anti-bonding cation-anion electronic states at lower binding energy is beneficial for hole formation, which means that the electron transition is facilitated. Therefore, with such electronic structure, $BiPO_4$ will be a good electron donor. On the other hand, as a halogen compound, BiOI has stronger electron affinity, which makes it a relatively good electron acceptor, accepting the electrons from $BiPO_4$ more easily. As a result, charge transfer transition between $BiPO_4$ and BiOI is possible and this charge transfer absorption takes place in the range of 520–620 nm. However, charge transfer absorption was only observed when the ratio of $BiPO_4$ were 7% and 10%, whereas it did not apply to 3% and 15% samples. This may be explained as follows: it is supposed that like d-d charge transfer transitions in transition metals, the charge transfer absorption in composite photocatalyst is vulnerable to

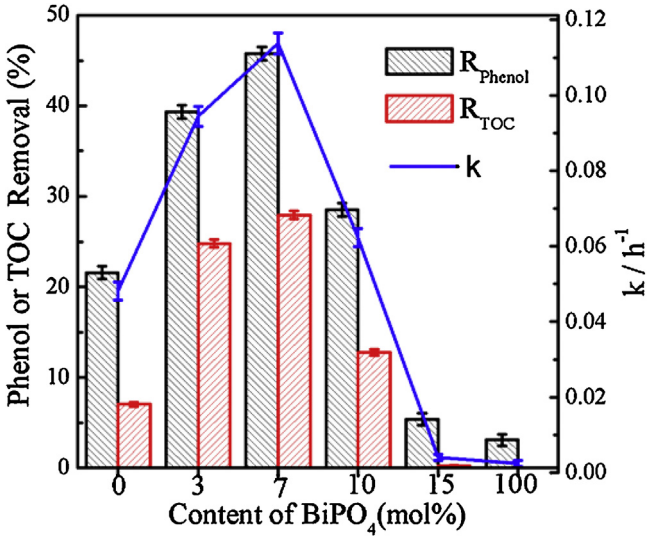

Fig. 3. Visible light photocatalytic activity of $BiPO_4$/BiOI with different content of $BiPO_4$.

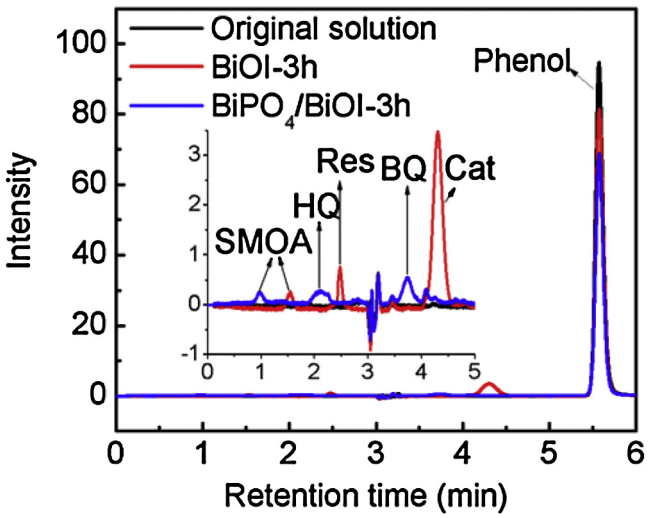

Fig. 4. HPLC spectrums of phenol solution degraded by BiOI or $BiPO_4$/BiOI under visible light.

environmental factors. When the ratio of $BiPO_4$ is small (3%), there may be fewer $BiPO_4$ nanorods that can form intimate interaction with BiOI, leading to the charge transfer absorption too weak to be observed. When the amount of $BiPO_4$ increases to 15%, the absorption edge of $BiPO_4$/BiOI suffers from an obvious blue shift compared with BiOI. This may be caused by the formation of solid solution. As is reported $(AgIn)_xZn_{2(1-x)}S_2$ solid solution formed when the raw materials of ZnS and $AgInS_2$ were treated simultaneously and its band gap was narrower compared with the original wide band gap component semiconductor[42], which was similar to our result. Therefore, it is supposed that the composite photocatalyst has changed into solid solution when the mole ratio of $BiPO_4$ is 15%. As a result, the charge transfer absorption is not observed on this sample.

3.2. Enhancement of photocatalytic activity

The photocatalytic activity of the $BiPO_4$/BiOI composites was evaluated by degradation of phenol. Fig. 3 showed the relationship of the apparent rate reaction constant (k) and the removal percentage of phenol and TOC with the content of $BiPO_4$. Compared with pure BiOI, the photocatalytic activity of $BiPO_4$/BiOI firstly increased then decreased as the mole content of $BiPO_4$ increased from 3% to 15%. The k reached the highest value when the mole content of $BiPO_4$ was 7%, and it was about 2 times as high as that of pure BiOI. After 5 h of visible light irradiation, the removal percentage of phenol by pure BiOI was 21.6%, and it was 45.8% by $BiPO_4$/BiOI composite (7%), which was about 2 times as high as that of pure BiOI. However, the removal percentage of TOC by pure BiOI was 7.0%, while it was 27.9% by $BiPO_4$/BiOI composite (7%), which was about 4 times as high as that of pure BiOI. Similarly, compared with pure BiOI, the intensified factor for removal percentage of TOC by $BiPO_4$/BiOI-3% and 10% was larger than that for the removal percentage of phenol. This revealed that the mineralization ability of $BiPO_4$/BiOI composite was stronger than that of pure BiOI. This conclusion could be proved by the HPLC result (Fig. 4). After 3 h of visible light irradiation, some small molecular organic acids (SMOA) [43] formed in the photocatalytic degradation process of phenol by both pure BiOI and $BiPO_4$/BiOI composite. This suggested that both of the two photocatalysts could degrade phenol partially by cleaving phenyl to form small molecular organic acids, resulting in the decline of TOC [44]. However, large amount of catechol (Cat) [25] formed and could not be degraded rapidly by pure BiOI, and small amount of resorcinol (Res) [43] also existed. By comparison, only small amount of hydroquinone (HQ) and benzoquinone (BQ) [43] remained as the conversion intermediate when phenol was degraded by $BiPO_4$/BiOI composite. Catechol was not detected when $BiPO_4$/BiOI composite was used to degrade phenol, indicating that $BiPO_4$/BiOI composite could degrade it rapidly. This meant that the mineralization ability of pure BiOI was relatively weak and it was not able to degrade some intermediates rapidly. By comparison, the oxidation ability of $BiPO_4$/BiOI composite was enhanced. It could degrade the intermediates rapidly, resulting in the faster removal rate of TOC. Therefore, conclusion can be drawn that the combination of $BiPO_4$ and BiOI could not only increase the apparent rate constant, but also enhance the mineralization ability, which enabled $BiPO_4$/BiOI composite to efficiently remove the TOC of the pollution system. In order to find out the stability of $BiPO_4$/BiOI composite photocatalyst, cyclic degradation experiment was conducted. After each photocatalysis degradation experiment, the photocatalyst was separated via centrifugation and was subsequently washed with distilled water before reuse. As can be seen from Fig. S4, the photocatalytic activity of $BiPO_4$/BiOI in the second round decreased the most and after that, it did not show significant decrease. The removal percentages of phenol were 45.8%, 37.6%, 34.2% and 32.1% after 5 h in the 4 successive cycles, respectively. The largest decrease of the removal percentage in the second round may be caused by the decreased ability to adsorb phenol after the first round. Therefore, it can be concluded that the $BiPO_4$/BiOI composite photocatalyst was relatively stable as a whole but its stability still needs further improvement.

Photocurrent is an effective method to reflect the generation, separation and migration efficiency of photogenerated carriers. It can be seen from Fig. 5 that as the content of $BiPO_4$ increased, the photocurrent firstly increased then decreased (except for the 15% composite), which had a positive correlation with the photocatalytic activity on the whole. An exception was the 15% one, which had higher photocurrent but lower photocatalytic activity. This may be caused by the formation of solid solution, which has better conductivity than the original components. This improved conductivity (electron mobility: an important factor that influences photocurrent but has no effect on photocatalytic oxidation activity) will enhance the photocurrent, while it will not have any effect on its photocatalytic oxidation activity. Therefore, although $BiPO_4$/BiOI-15% possesses higher photocurrent than $BiPO_4$/BiOI-10%, its photocatalytic activity is lower than the latter one.

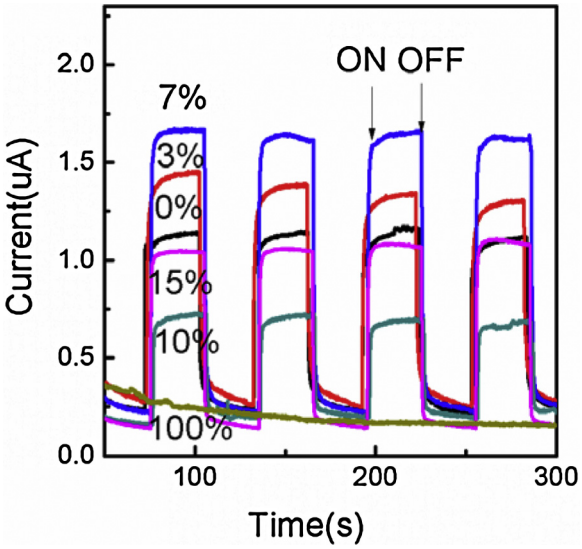

Fig. 5. Visible light photocurrent of $BiPO_4$/BiOI with different content of $BiPO_4$.

Wavelength dependent photocurrent was also measured in order to know the relationship between the photo-to-current conversion efficiency and the incident light wavelength. As shown in Fig. 6, the photocurrents of $BiPO_4$/BiOI (7%) were all higher than that BiOI when the cut-off wavelength was smaller than 550 nm. This result revealed the improved photo-to-current conversion efficiency of the composite photocatalyst under the illumination of visible light with shorter wavelengths, which had higher energy. This is consistent with the enhanced mineralization ability. However, when the wavelength of the incident light was equal to or longer than 550 nm, the photocurrent of $BiPO_4$/BiOI (7%) became smaller than that of pure BiOI, which may be caused by its decreased absorption ability for longer wavelength light.

3.3. Mechanism of the enhanced photocatalytic activity

The photocatalytic activity is closely related with the generation, separation, migration efficiency and the oxidation–reduction ability of the photogenerated carriers [45]. As mentioned above, the photocurrent had a positive correlation with the photocatalytic activity, which meant that the improvement of the generation, separation and migration efficiency of photogenerated carriers was

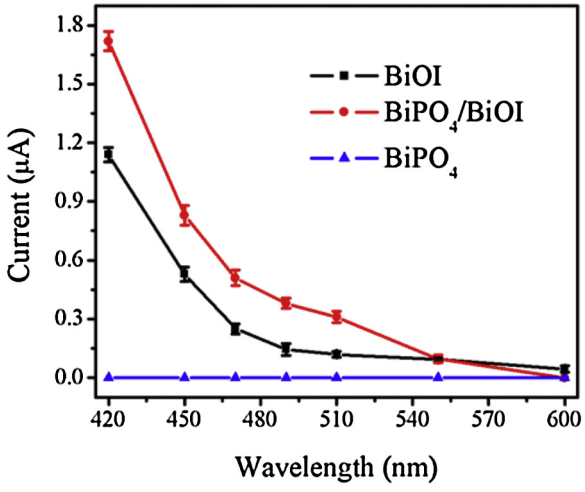

Fig. 6. Wavelength dependent photocurrent of pure $BiPO_4$, pure BiOI and $BiPO_4$/BiOI-7%.

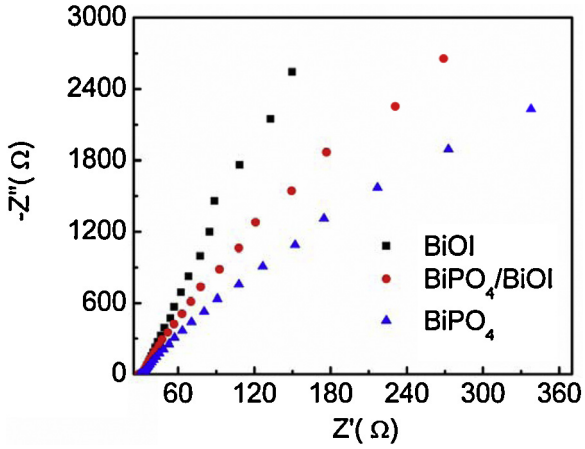

Fig. 7. Nyquist plots for pure BiOI, pure $BiPO_4$ and $BiPO_4$/BiOI under visible light.

an important factor for the increased photocatalytic activity. The UV–vis DRS revealed that the visible light absorption ability of $BiPO_4$/BiOI composite was lower than that of pure BiOI, which was not favorable for the generation of photogenerated carriers. Therefore, the enhancement of photocurrent was mainly induced by the increased separation and migration efficiency of photogenerated carriers. The interface charge separation efficiency could be investigated by the electrochemical impedance spectra (Nyquist plots) [46]. The smaller the arc radius is, the higher the efficiency of charge transfer is. Fig. 7 showed that the radius of $BiPO_4$ was the smallest among the three samples, implying that the charge transfer efficiency of $BiPO_4$ was the highest. The fast charge transfer rate of $BiPO_4$ was attributed to its large dipole moment, which could promote the separation of electrons and holes [47]. The radius of $BiPO_4$/BiOI was smaller than that of pure BiOI, implying that the charge transfer efficiency of $BiPO_4$/BiOI composite was higher than that of pure BiOI. Therefore, it could be concluded that the existence of $BiPO_4$ could accelerate the separation and migration efficiency of photogenerated carriers. However, as the size of $BiPO_4$ increased, the ratio of the contact area of $BiPO_4$ and BiOI to the whole area of $BiPO_4$ decreased. This would decrease the interaction of $BiPO_4$ and BiOI and it was not favorable for the enhancement of separation efficiency of photogenerated carriers. As a result, the photocatalytic activity of $BiPO_4$/BiOI composite decreased when the content of $BiPO_4$ was too high.

The degradation of organic pollutants is processed through oxidation and reduction reaction, whose rate mainly depends on the kind of oxidative species and the amount of them. The kind and the amount of the oxidative species can be detected through trapping experiment. EDTA-2Na was used as hole scavenger and t-BuOH as hydroxyl radical scavenger [48,49]. The role that the hole and the hydroxyl radical played can be identified by observing their effect on the photocatalytic reaction rate. Purging N_2 into the solution could make an anaerobic environment by purging the O_2 out, which would prohibit the formation of superoxide radical ($^{\bullet}O_2^-$). So N_2 is a good detective molecular to make certain the effect of $^{\bullet}O_2^-$. It could be seen from the result (Fig. S3) that EDTA-2Na could significantly decrease the photocatalytic activity of both pure BiOI and $BiPO_4$/BiOI composite. N_2 had less effect on them, and t-BuOH had the least effect. This implied that photogenerated holes were the main active species for both pure BiOI and $BiPO_4$/BiOI composite to degrade phenol. $^{\bullet}O_2^-$ was also an important factor and hydroxyl radical was a minor active species in the degradation process of phenol. The valence band positions of both pure BiOI and $BiPO_4$/BiOI composite were low, thus the photogenerated holes had strong oxidation ability and they could degrade phenol through hole oxidation mechanism. Theoretically speaking, the conduction

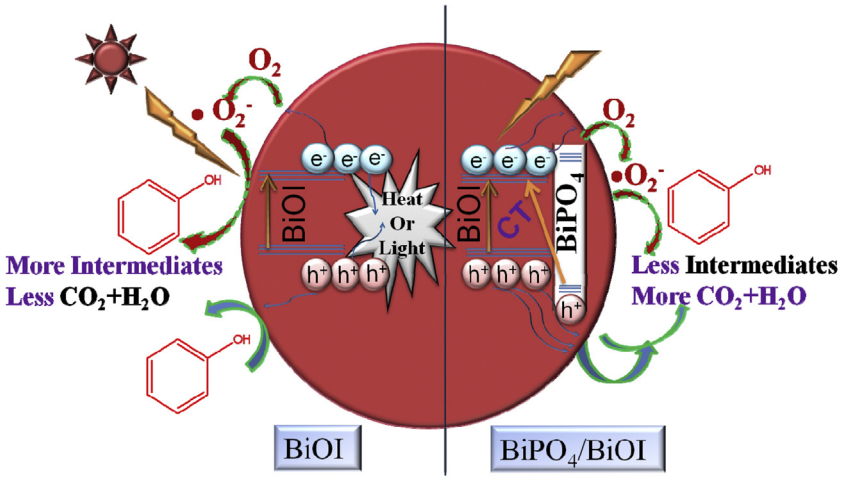

Fig. 8. The proposed degradation mechanism of phenol by pure BiOI and $BiPO_4$/BiOI composite.

band minimum (CBM) of BiOI was low, so the photogenerated electrons on the CBM were not reductive enough to reduce O_2 and form $•O_2^-$. It was reported that the excitation of BiOI with high energy light (λ = 400 or 508 nm) could result in the photogenerated electrons exciting up to a reformed higher CBM potential than E^0 (O_2/$•O_2^-$) (−0.046 eV), thus they could react with O_2 to produce $•O_2^-$ [10]. Therefore, BiOI could degrade many organic pollutants through $•O_2^-$ [50]. It could be seen from the trapping experiments that the active species were the same for BiOI and $BiPO_4$/BiOI, and the main active species for them were photogenerated holes. The UV-vis DRS revealed that there was charge transfer absorption between $BiPO_4$ and BiOI in $BiPO_4$/BiOI composite photocatalyst. This resulted in the formation of more oxidative photogenerated holes in the valance band of $BiPO_4$. The enhanced oxidation ability of photogenerated holes of $BiPO_4$/BiOI composite might account for the faster removal rate of TOC and the formation of fewer degradation intermediates of phenol. Therefore, $BiPO_4$/BiOI composite was more efficient in degrading and mineralizing phenol through hole oxidation mechanism.

Based on the above results and analysis, the degradation mechanism of phenol by pure BiOI and $BiPO_4$/BiOI composite was illustrated in Fig. 8. On the one hand, the hole generated by pure BiOI under visible light irradiation could transfer phenol to its intermediates or directly to CO_2 and H_2O. On the other hand, the photogenerated electrons with higher energy could react with O_2 to form $•O_2^-$, and then transfer phenol to its intermediates. However, the recombination rate of the electrons and holes produced by pure BiOI was fast, resulting in the low photocatalytic activity. After its combination with $BiPO_4$, the hole generated via charge transfer possessed stronger oxidation ability, which significantly enhanced the mineralization ability of $BiPO_4$/BiOI composite, resulting in the formation of fewer degradation intermediates and enhanced removal rate of TOC. Besides, the dipole moment of $BiPO_4$ is large. It has been proved that the large dipole moment could promote the charge separation [51]. Therefore, the existence of $BiPO_4$ could enhance the photocatalytic activity by accelerating the separation and migration rate of photogenerated electrons and holes.

4. Conclusions

In summary, $BiPO_4$/BiOI composite photocatalyst was synthesized via a facile anion exchange method. The visible light mineralization ability of $BiPO_4$/BiOI was improved via charge transfer. This composite photocatalyst is superior to $BiPO_4$ since it is visible light responsive, whereas $BiPO_4$ can only respond to UV light. More importantly, the mineralization ability of $BiPO_4$/BiOI semiconductor is stronger than BiOI due to the formation of more oxidative holes induced by the charge transfer between $BiPO_4$ donor and BiOI acceptor. The relatively large dipole moment of $BiPO_4$ could promote the separation and migration of the photogenerated electrons and holes. This improved separation and migration efficiency of photogenerated carriers, together with the enhanced mineralization ability of the photogenerated holes in $BiPO_4$/BiOI composite photocatalyst, resulted in its improved removal efficiency for phenol and TOC under visible light (λ > 420 nm) irradiation, which were about 2 and 4 times as high as that of pure BiOI, respectively. This study may provide new insights for the understanding of enhanced mineralization ability of composite photocatalysts, and may also pave the way for the design of efficient visible light photocatalytic systems.

Acknowledgements

This work was partly supported by National Basic Research Program of China (2013CB632403), National High Technology Research and Development Program of China (2012AA062701), National Natural Science Foundation of China (21373121 and 51102150).

Appendix A. Supplementary data

Supplementary data associated with this article can be found, in the online version, at http://dx.doi.org/10.1016/j.apcatb.2014.08.039.

References

[1] T. Ochiai, A. Fujishima, J. Photochem. Photobiol. C 13 (2012) 247–262.
[2] H. Park, Y. Park, W. Kim, W. Choi, J. Photochem. Photobiol. C 15 (2013) 1–20.
[3] S. Baruah, M. Jaisai, J. Dutta, Catal. Sci. Technol. 2 (2012) 918–921.
[4] A. Fujishima, X. Zhang, D.A. Tryk, Surf. Sci. Rep. 63 (2008) 515–582.
[5] H.G. Yu, R. Liu, X.F. Wang, P. Wang, J.G. Yu, Appl. Catal. B: Environ. 111 (2012) 326–333.
[6] S.W. Liu, K. Yin, W.S. Ren, B. Cheng, J.G. Yu, J. Mater. Chem. A 22 (2012) 17759–17767.
[7] Y. Lv, Y. Zhu, Y. Zhu, J. Phys. Chem. C 117 (2013) 18520–18528.
[8] Y. Lv, Y. Liu, Y. Zhu, Y. Zhu, J. Mater. Chem. A 2 (2014) 1174–1182.
[9] R.A. He, S.W. Cao, P. Zhou, J.G. Yu, Chin. J. Catal. 35 (2014) 989–1007.
[10] L. Ye, J. Chen, L. Tian, J. Liu, T. Peng, K. Deng, L. Zan, Appl. Catal. B: Environ. 130 (2013) 1–7.
[11] X. Qin, H. Cheng, W. Wang, B. Huang, X. Zhang, Y. Dai, Mater. Lett. 100 (2013) 285–288.
[12] W. Zhang, Q. Zhang, F. Dong, Ind. Eng. Chem. Res. 52 (2013) 6740–6746.
[13] A. Santos, P. Yustos, A. Quintanilla, F. Garcia-Ochoa, J.A. Casas, J.J. Rodriguez, Environ. Sci. Technol. 38 (2004) 133–138.

[14] L. Chen, D. Jiang, T. He, Z. Wu, M. Chen, CrystEngComm 15 (2013) 7556–7563.
[15] H. Cheng, W. Wang, B. Huang, Z. Wang, J. Zhan, X. Qin, X. Zhang, Y. Dai, J. Mater. Chem. A 1 (2013) 7131–7136.
[16] P. Li, X. Zhao, C.J. Jia, H. Sun, L. Sun, X. Cheng, L. Liu, W. Fan, J. Mater. Chem. A 1 (2013) 3421–3429.
[17] K.H. Reddy, S. Martha, K.M. Parida, Inorg. Chem. 52 (2013) 6390–6401.
[18] G. Dai, J. Yu, G. Liu, J. Phys. Chem. C 115 (2011) 7339–7346.
[19] J. Jiang, X. Zhang, P. Sun, L. Zhang, J. Phys. Chem. C 115 (2011) 20555–20564.
[20] T.B. Li, G. Chen, C. Zhou, Z.Y. Shen, R.C. Jin, J.X. Sun, Dalton Trans. 40 (2011) 6751–6758.
[21] L. Yang, S. Luo, Y. Li, Y. Xiao, Q. Kang, Q. Cai, Environ. Sci. Technol. 44 (2010) 7641–7646.
[22] M. Deo, D. Shinde, A. Yengantiwar, J. Jog, B. Hannoyer, X. Sauvage, M. More, S. Ogale, J. Mater. Chem. A 22 (2012) 17055–17062.
[23] C.S. Pan, Y.F. Zhu, Environ. Sci. Technol. 44 (2010) 5570–5574.
[24] Y.F. Liu, X.G. Ma, X. Yi, Y.F. Zhu, Acta Phys. Chim. Sin. 28 (2012).
[25] Y.F. Liu, Y.Y. Zhu, J. Xu, X.J. Bai, R.L. Zong, Y.F. Zhu, Appl. Catal. B: Environ. 142–143 (2013) 561–567.
[26] C.S. Pan, J. Xu, Y.J. Wang, D. Li, Y.F. Zhu, Adv. Funct. Mater. 22 (2012) 1518–1524.
[27] Z. Li, S. Yang, J. Zhou, D. Li, X. Zhou, C. Ge, Y. Fang, Chem. Eng. J. 241 (2014) 344–351.
[28] T. Lv, L. Pan, X. Liu, Z. Sun, RSC Adv. 2 (2012) 12706–12709.
[29] H. Lin, H. Ye, B. Xu, J. Cao, S. Chen, Catal. Commun. 37 (2013) 55–59.
[30] S. Wu, H. Zheng, Y. Lian, Y. Wu, Mater. Res. Bull. 48 (2013) 2901–2907.
[31] J. Cao, B. Xu, H. Lin, S. Chen, Chem. Eng. J. 228 (2013) 482–488.
[32] Y.G. Zuo, J. Hoigne, Environ. Sci. Technol. 26 (1992) 1014–1022.
[33] P. Borer, B. Sulzberger, S.J. Hug, S.M. Kraemer, R. Kretzschmar, Environ. Sci. Technol. 43 (2009) 1871–1876.
[34] J. Xu, J. Li, F. Wu, Y. Zhang, Environ. Sci. Technol. 48 (2014) 272–278.
[35] T. Paul, M.L. Machesky, T.J. Strathmann, Environ. Sci. Technol. 46 (2012) 11896–11904.
[36] D. Zhu, S. Hyun, J.J. Pignatello, L.S. Lee, Environ. Sci. Technol. 38 (2004) 4361–4368.
[37] P. Le Magueres, S.M. Hubig, S.V. Lindeman, P. Veya, J.K. Kochi, J. Am. Chem. Soc. 122 (2000) 10073–10082.
[38] K. Vandewal, A. Gadisa, W.D. Oosterbaan, S. Bertho, F. Banishoeib, I. Van Severen, L. Lutsen, T.J. Cleij, D. Vanderzande, J.V. Manca, Adv. Funct. Mater. 18 (2008) 2064–2070.
[39] S. Few, J.M. Frost, J. Kirkpatrick, J. Nelson, J. Phys. Chem. C 118 (2014) 8253–8261.
[40] K. Liu, Y. Yao, Y. Liu, C. Wang, Z. Li, X. Zhang, Langmuir 28 (2012) 10697–10702.
[41] A. Walsh, Y. Yan, M.N. Huda, M.M. Al-Jassim, S.-H. Wei, Chem. Mater. 21 (2009) 547–551.
[42] I. Tsuji, H. Kato, H. Kobayashi, A. Kudo, J. Am. Chem. Soc. 126 (2004) 13406–13413.
[43] L. Liu, H. Liu, Y.-P. Zhao, Y. Wang, Y. Duan, G. Gao, M. Ge, W. Chen, Environ. Sci. Technol. 42 (2008) 2342–2348.
[44] J.B. Zhang, J. Zhuang, L.Z. Gao, Y. Zhang, N. Gu, J. Feng, D.L. Yang, J.D. Zhu, X.Y. Yan, Chemosphere 73 (2008) 1524–1528.
[45] H. Tong, S.X. Ouyang, Y.P. Bi, N. Umezawa, M. Oshikiri, J.H. Ye, Adv. Mater. 24 (2012) 229–251.
[46] H. Liu, S.A. Cheng, M. Wu, H.J. Wu, J.Q. Zhang, W.H. Li, C.N. Cao, J. Phys. Chem. A 104 (2000) 7016–7020.
[47] C.S. Pan, D. Li, X.G. Ma, Y. Chen, Y.F. Zhu, Catal. Sci. Technol. 1 (2011) 1399–1405.
[48] H. Zhang, R.L. Zong, J.C. Zhao, Y.F. Zhu, Environ. Sci. Technol. 42 (2008) 3803–3807.
[49] L. Yang, L.E. Yu, M.B. Ray, Environ. Sci. Technol. 43 (2009) 460–465.
[50] X. Li, C. Niu, D. Huang, X. Wang, X. Zhang, G. Zeng, Q. Niu, Appl. Surf. Sci. 286 (2013) 40–46.
[51] J. Sato, H. Kobayashi, Y. Inoue, J. Phys. Chem. B 107 (2003) 7970–7975.